

Universal Trajectories of Motile Particles Driven by Chemical Activity

Chaouqi Misbah,^{1,*} Suhail M. Rizvi,^{1,2} Wei-Fan Hu,³ Te-Sheng Lin,⁴ Salima Rafai,¹ and Alexander Farutin¹

¹*Univ. Grenoble Alpes, CNRS, LIPhy, F-38000 Grenoble, France*

²*Current address: Department of Biomedical Engineering,
Indian Institute of Technology Hyderabad, Sangareddy, Telangana 502285, India*

³*Department of Mathematics, National Central University, 300 Zhongda Road, Taoyuan 320, Taiwan*

⁴*Department of Applied Mathematics, National Chiao Tung University, 1001 Ta Hsueh Road, Hsinchu 300, Taiwan*

Locomotion is essential for living cells. It enables bacteria and algae to explore space for food, cancer to spread, and immune system to fight infections. Motile cells display trajectories of intriguing complexity, from regular (e.g. circular, helical, and so on) to irregular motions (run-tumble), the origin of which has remained elusive for over a century. This dynamics versatility is conventionally attributed to the shape asymmetry of the motile entity, to the suspending media, and/or to stochastic regulation. We propose here a universal approach highlighting that these movements are generic, occurring for a large class of cells and artificial microswimmers, without the need of invoking shape asymmetry nor stochasticity, but are encoded in their inherent nonlinear evolution. We show, in particular, that for a circular and spherical particle moving in a simple fluid, circular, helical and chaotic motions (akin to a persistent random walk) emerge naturally in different regions of parameter space. This establishes the operating principles for complex trajectories manifestation of motile systems, and offers a new vision with minimal ingredients. The reduced evolution equations based on symmetries are consistent with those derived for a model of an autophoretic particle including diffusion, emission/absorption at the particle surface and hydrodynamics, and provide qualitative and quantitative agreement.

arXiv:2112.13801v1 [cond-mat.soft] 27 Dec 2021

* chaouqi.misbah@univ-grenoble-alpes.fr

Introduction. Cells range in size from a micrometer for a bacterium to a few dozen micrometers for eukaryotic cells. The physics of their movement is thus dominated by the viscosity of water. They have specialized structures, the flagella or cilia, whose movements are maintained by complex biochemical mechanisms. There is also increasing evidence that non flagellated eukaryotic cells that have long been assumed to require a substrate for migration (crawling) can actually swim[1–4] in a fluid (fluid crawling). One common feature of motile microorganisms is their random-like trajectories sometimes qualified as run-and-tumble [5–9] which constitutes a potential optimal way to span the space for survival.

In the seminal work of Jennings (1901)[10], many microorganisms such as zoospores, flagellate and ciliated Protista are shown to swim in spiral. It is now well established that curved trajectories, such as spiral, circular and helical, are ubiquitous in nature[11–15] as well as for synthetic non Brownian microswimmers [16–21]. The occurrence of such curved trajectories is conventionally retrieved in theoretical models by either invoking stochasticity of the system, chirality of the motile particle, a surrounding non Newtonian fluid or the presence of bounding walls [11, 13–15, 17, 19–22].

The present goal is to propose a generic theory, based on symmetry arguments, that produce observed run and tumble trajectories as well as circular, helical and chaotic trajectories. The tour de force here is that these non linear features are obtained for spherical particles moving in an isotropic medium in a deterministic manner. The symmetry breaking emerges here from the intrinsic non linearities of the problem and thus do not have to be introduced in an *ad hoc* manner.

Model. We consider a swimmer powered by a scalar field, say a concentration field c which evolves in space and time. Marangoni-driven particles [23–25], and acto-myosin assisted cell motility [3, 26, 27] are two typical examples. In these explicit examples the concentration fields obey advection-diffusion equations, with boundary conditions (such as chemical emission at the particle surface, etc...), which are coupled to hydrodynamics (swimming) or friction (crawling) equations.

A common feature of motile systems powered by a chemical field is the occurrence of a spontaneous symmetry-breaking [3, 23–27] (concentration polarity) leading to autonomous swimming. For the sake of simplicity let us begin with a 2D configuration where the particle has a circular shape with radius unity.

Before presenting the reduced version of dynamics (in terms of two Fourier modes) based on symmetries, we would like first to outline how these equations can be obtained from a full model of an autophoretic particle. The model consists [23] of a rigid a particle (taken to be a circle with radius a), which emits/absorbs a solute that diffuses and is advected by the flow. In a reduced form the model takes the form [23]

$$\frac{\partial c}{\partial t} + \mathbf{u} \cdot \nabla c = \frac{1}{Pe} \Delta c, \quad \Delta \mathbf{u} - \nabla p = \mathbf{0}, \quad \nabla \cdot \mathbf{u} = 0, \quad (1)$$

with boundary conditions

$$\frac{\partial c}{\partial r}(1, \theta, t) = -A, \quad \mathbf{u}(1, \theta) = M \nabla_s c \quad (2)$$

\mathbf{u} and p is the velocity and pressure fields, and η is the fluid viscosity. Péclet number is defined by $Pe = |\mathcal{A}\mathcal{M}|a/D^2$, where D is the diffusion constant, $A = \mathcal{A}/|\mathcal{A}| = \pm 1$ is the dimensionless emission rate ($A > 0$: emission, $A < 0$: adsorption), and $M = \mathcal{M}/|\mathcal{M}|$ is the dimensionless particle mobility. Due to the logarithmic divergence of concentration field in 2D, the size is taken to be finite, so that that the boundary condition for the concentration field is $c(R, \theta, t) = 0$ (see discussion in 3D below),

The velocity field can be expressed as $\mathbf{u} = (\frac{1}{r} \frac{\partial \psi}{\partial \theta}, -\frac{\partial \psi}{\partial r})$ (in polar components), where ψ is the stream function and has the following analytical form [28, 29]

$$\psi(r, \theta, t) = \sum_{\ell=-\infty}^{\infty} \frac{1-r^2}{2r^{|\ell|}} ikMc_{\ell}(1, t)e^{i\ell\theta}, \quad (3)$$

where we have used the boundary condition $\mathbf{u}(1, \theta) = M \nabla_s c$ to express the series coefficients in terms of c . Inserting (3) into diffusion equation (Eq.(1)) we obtain a closed nonlinear equation for $c(\mathbf{r}, t)$

$$\frac{\partial c(\mathbf{r}, t)}{\partial t} = \sum_k \frac{c_k(1, t)Me^{ik\theta}}{2r^{|k|+1}} \left[(r^2 - 1)k^2 \frac{\partial c(\mathbf{r}, t)}{\partial r} + ik(2r^2 + (1 - r^2)|k|) \frac{\partial c(\mathbf{r}, t)}{\partial \theta} \right] + \frac{1}{Pe} \Delta c(\mathbf{r}, t) \quad (4)$$

A stationary solution where there is no net flow and zero phoretic velocity exists at all Péclet numbers with the solute concentration $c_0(r) = \ln(R/r)$. In general c can be written as $c(r, \theta, t) = \sum_{\ell=-\infty}^{\infty} \hat{c}_{\ell}(r, t)e^{i\ell\theta}$. Neglecting higher

order but linear terms, the following relation for the Fourier mode \hat{c}_ℓ is obtained:

$$\frac{\partial c_\ell}{\partial t} = -AM\ell^2 \frac{1-r^2}{2r^{|\ell|+2}} c_\ell(1,t) + \frac{1}{Pe} \left(\frac{\partial^2}{\partial r^2} + \frac{1}{r} \frac{\partial}{\partial r} - \frac{k^2}{r^2} \right) c_\ell(r,t). = \hat{L}_\ell(Pe)c_\ell \quad (5)$$

where \hat{L}_ℓ is the linear operator. Looking for solutions in the form $c_\ell = f_\ell(r)e^{i\sigma t}$, previous calculations[21, 23] showed that $\sigma_\ell \sim (Pe - Pe_\ell)$, where Pe_ℓ is the critical Péclet number for which the ℓ -th harmonic becomes unstable. It has also been shown that the first harmonic ($\ell = 1$) becomes first unstable. By increasing Pe the second harmonic becomes also unstable, and so on. We assume that $Pe - Pe_\ell$ is small close enough, where Pe_ℓ is the critical Péclet number for instability of ℓ -th harmonic. This is just a formal requirement that allows us to keep dynamics only of these two harmonics. It will be shown that retaining only these two modes is sufficient to exhibit a large panel of behavior going from straight to chaotic motion.

The full equation (4) can be, by using Fourier decomposition with respect to θ , rewritten as

$$\begin{aligned} \frac{\partial c_\ell(r,t)}{\partial t} &= \sum_{m \neq \ell} \frac{mc_m(1,t)M}{2r^{|m|+1}} \left[(r^2 - 1)m \frac{\partial c_{\ell-m}(r,t)}{\partial r} + (m - \ell)(2r^2 + (1 - r^2)|m|)c_{\ell-m}(r,t) \right] + \hat{L}_\ell(Pe_\ell)c_\ell(r,t) \\ &+ (\hat{L}_\ell(Pe) - \hat{L}_\ell(Pe_\ell))c_\ell(r,t) \equiv Q(r,t) + \hat{L}_\ell(Pe_\ell)c_\ell(r,t) \end{aligned} \quad (6)$$

The approach is thus to write

$$c_l(r,t) = C_l(t)f_{l,0}(r) + \delta c_l(r,t) \quad l \in \{1,2\}, \quad (7)$$

where $C_l(t)$ is the complex amplitude, $f_{l,0}(r)$ is the proper function such that $\hat{L}_l(Pe_{\ell,c})f_{l,0}(r) = 0$, and $\delta c_l(r,t)$ is a projection of the function $c_l(r,t)$ on the space of all other proper functions of the operator $\hat{L}_l(Pe_l)$:

$$\delta c_l(r,t) = \sum_{k>0} C_{l,k}(t)f_{l,k}(r), \quad \hat{L}_l(Pe_l)f_{l,k}(r) = \lambda_{l,k}f_{l,k}(r). \quad (8)$$

Here the functions $f_{l,k}(r)$ are the proper functions of the operator $\hat{L}_l(Pe_l)$ corresponding to eigenvalues $\lambda_{l,k}$. Equation(6) becomes then

$$\partial_t C_\ell f_{\ell,0}(r) = \hat{L}_\ell(Pe_\ell)\delta c_\ell(r,t) + \tilde{Q}(r,t) - \partial_t \delta c_\ell(r,t). \quad (9)$$

where \tilde{Q} is obtained from Q in which we substitute $c_\ell(r,t)$ by $C_\ell(t)f_{l,0}(r) + \delta c_\ell(r,t)$

The goal now is to obtain closed equations for $C_1(t)$ and $C_2(t)$. Close enough to bifurcation these amplitude are small, $C_1 = O(\epsilon)$ and $C_2 = O(\epsilon)$, where ϵ , measures distance from criticality, $|Pe - Pe_\ell| = O(\epsilon)$. Since the growth rate is small, $\sigma_\ell \sim |Pe - Pe_\ell| = O(\epsilon)$, we also have $\partial_t C_\ell = O(\epsilon^2)$ (usual Landau critical slowing down). Higher order harmonics amplitudes are smaller; for $l > 2$, we have $c_l(r,t) = O(\epsilon^{\lceil l/2 \rceil})$ and $\partial_t c_l(r,t) = O(\epsilon^{\lceil l/2 \rceil + 1})$. This implies $\delta c_\ell(r,t) = O(\epsilon^2)$ and $\partial_t \delta c_\ell(r,t) = O(\epsilon^3)$. $\delta c_\ell(r,t)$ induces cubic terms, meaning that it does not enter the evolution equations of C_ℓ to order ϵ^2 . The evolution equations can be readily obtained thanks to the Fredholm alternative theorem. For that we need to determine the kernel of the adjoint operator $\hat{L}_l^+(Pe_l)$:

$$\hat{L}_l^+(Pe_l)g_{\ell,0}(r) = 0, \quad (10)$$

The adjoint operator is defined with respect to the inner product

$$\langle f, g \rangle = \int_1^R f(r)g(r)^* r dr, \quad (11)$$

which is chosen to maintain the self-adjoint property of the diffusion operators \hat{D}_l subject to the boundary conditions of the functions $c_l(r)$. By construction δc_ℓ satisfies $\langle g_{\ell,0}, \delta c_\ell \rangle = 0$.

By projecting Eq. (9) on $g_{\ell,0}$ function we obtain the desired equation for C_ℓ , which formally reads

$$\partial_t C_\ell = \frac{\langle \tilde{Q}(r,t), g_{\ell,0} \rangle}{\langle f_{\ell,0}, g_{\ell,0} \rangle} \quad (12)$$

Using $c_l(r,t) = C_l(t)f_{l,0}(r)$ and collecting in \tilde{Q} terms involving $C_1(t)$ and $C_2(t)$ (higher harmonics are supposed to be stable) we straightforwardly obtain the form of the evolution equations for $C_1(t)$ and $C_2(t)$ (which factor out of scalar

products) to quadratic order, where coefficients are scalar products involving $f_{\ell,0}(r)$ and $g_{\ell,0}(r)$. These functions can even be determined and the scalar products can be evaluated analytically (see [30]; since our goal here is to prove the form of the equations, the values of coefficients are unimportant for our purposes).

$$\begin{aligned}\dot{C}_1 &= \sigma_1 C_1 + \beta_1 C_1^* C_2 \\ \dot{C}_2 &= \sigma_2 C_2 - \beta_2 C_1^2\end{aligned}\tag{13}$$

It turns out that the cubic terms are necessary for the nonlinear saturation, this is why $\delta c_\ell(r, t)$ must be taken into account, and we obtain [30]

$$\begin{aligned}\dot{C}_1 &= \sigma_1 C_1 + \beta_1 C_1^* C_2 - \gamma_1 |C_2|^2 C_1 \\ \dot{C}_2 &= \sigma_2 C_2 - \beta_2 C_1^2 - \gamma_2 |C_1|^2 C_2 - \xi_2 |C_2|^2 C_2\end{aligned}\tag{14}$$

The various coefficients obtained for the phoretic model are given in [30].

Nonlinear evolution equations from symmetries. The forms of the above set of equations (14) are in fact quite general and do not depend on the explicit model (only the values of the coefficients depend on the model).

The form of nonlinear evolution equations must comply with space symmetry. Indeed, due to particle and medium isotropy, a displacement along the bead periphery (rotation by a certain angle) by a constant amount θ_0 should leave the evolution equations invariant. The first Fourier mode reads as $c_1 \sim C_1(t)e^{i\theta} + c.c.$. If one changes θ by a constant θ_0 we have

$$\theta \rightarrow \theta + \theta_0 \implies C_1 \rightarrow C_1 e^{i\theta_0}\tag{15}$$

Rotation by constant angle is equivalent to a phase shift of c_1 .

More generally, since the evolution equations contains other harmonics, the evolution equations for $C_m(t)$ must be invariant under the transformation

$$C_m \rightarrow C_m e^{im\theta_0}\tag{16}$$

It is easy to check that the above set of equations (14) is invariant under transformation (16). Note that terms of the form C_1^2 , C_2^2 , for example, are not eligible, since they do not comply with the symmetry constraints. The set (14) is thus general and should be expected for any model driven by chemical activity (phoretic models, especially the one dealt with here, and motility driven by acto-myosin are two typical examples). It is also essential to note that the symmetry arguments do not depend on whether the particle is a swimmer, or crawler. For acto-myosin systems the appropriate dimensionless number is a dimensionless myosin contractility χ' (proportional to myosin contractility divided by viscosity and myosin diffusion) [3], instead of Pe . In that case motility takes place for χ' of order few unities, in consistent with experiments [3].

Due to the generic character of the equations for C_1 and C_2 we will below look at the model as general, and potentially applicable to various swimmers powered by a concentration field. Differences between systems will only show up in the values of the coefficients. In what follows we will exploit this generality without specific values of coefficients. Our goal is to establish what are the main features exhibited by Eqs. (14) by exploring different values of the coefficients. In Ref.[30] we can find the expressions of the coefficients for the above phoretic model, and where we show that the reduced model in terms of C_1 and C_2 captures both qualitatively and quantitatively the results of the full model.

Above we assumed that $C_2 = O(\epsilon)$ for a formal expansion in terms of ϵ . However, the set of equations (14) remain valid even if C_2 is of smaller order provided we decide to keep both C_1 and C_2 in the expansion without imposing the ϵ scaling. For example if C_2 is a sufficiently stable mode, its amplitude will be small. This happens if σ_2 is sufficiently negative, meaning that C_2 decays sufficiently fast to its steady state value. Using thus the adiabatic elimination of C_2 , (i.e. $\dot{C}_2 \simeq 0$) one obtains $C_2 = \beta_2 C_1^2 / \sigma_2$, and plugging it into (14) one obtains to leading order (cubic terms containing C_2 are of higher order)

$$\dot{C}_1 = \sigma_1 C_1 - \alpha_2 |C_1|^2 C_1\tag{17}$$

with $\alpha_2 = -\beta_2 \beta_1 / \sigma_2 > 0$ (supercritical bifurcation; subcritical bifurcations are not considered here). The nonlinear term is stabilizing and leads to saturation of the linear growth. Since $\sigma_2 < 0$, β_1 and β_2 must have the same sign (taken arbitrarily to be positive here; their sign is arbitrary, see below).

Since close to instability $\sigma_1 \sim (Pe - Pe_1)$, Eq. (17) has a steady state solution $C_1^{(0)} \sim (Pe - Pe_1)^{1/2}$, and the swimming speed (which is a linear function of C_1 ; see below) behaves in the same way with Pe :

$$v \equiv v^0 \sim (Pe - Pe_1)^{1/2}\tag{18}$$

The swimmer trajectory is straight. This is a signature of a supercritical bifurcation from non motile to motile state. This is in qualitative agreement with the numerical finding [21, 23].

When σ_2 becomes sufficiently small (of order ϵ), the second harmonic amplitude C_2 becomes comparable to C_1 , and dynamics is described by the full set (14). Note that a change $C_2 \rightarrow -C_2$ (corresponding to a phase shift of C_2 by π) leads to a simultaneous change of sign of β_1 and β_2 , this is why their sign is unimportant. The signs of cubic terms are dictated by the fact that nonlinear terms should saturate the linear growth of instability. That is $\gamma_1, \gamma_2, \xi_2 > 0$. It is always possible to set, for example ξ_2 , coefficient to unity upon an appropriate rescaling. σ_1 and σ_2 change sign at two different critical values of Pe , denoted as Pe_1 and Pe_2 .

Results. Setting $C_1 = \rho_1(t)e^{i\phi_1(t)}$ and $C_2 = \rho_2(t)e^{i\phi_2(t)}$ into (14) one obtains

$$\dot{\rho}_1 = \sigma_1\rho_1 + \beta_1\rho_1\rho_2 \cos(\Psi) - \gamma_1\rho_2^2\rho_1 \quad (19a)$$

$$\dot{\rho}_2 = \sigma_2\rho_2 - \beta_2\rho_1^2 \cos(\Psi) - \gamma_2\rho_1^2\rho_2 - \rho_2^3 \quad (19b)$$

$$\rho_2\dot{\Psi} = (\beta_2\rho_1^2 - 2\beta_1\rho_2^2) \sin(\Psi), \quad \Psi \equiv \phi_2 - 2\phi_1 \quad (19c)$$

The phases ϕ_1 and ϕ_2 are determined in terms of Ψ , ρ_1 and ρ_2 . For example, ϕ_1 obeys

$$\dot{\phi}_1 = \beta_1\rho_2 \sin(\Psi). \quad (20)$$

That only a single phase (Ψ) matters is a result of rotational invariance. The phase Ψ plays an important role in the occurrence of curved trajectory, and especially the circular one, which can be handled fully analytically. Since $c(s, t) = c_0 + \rho_1 e^{is+i\phi_1} + \rho_2 e^{2is+i\phi_2} + c.c.$ (in what follows c_0 will be omitted) we can write

$$c(s, t) = 2\rho_1 \cos(s + \phi_1) + 2\rho_2 \cos(2st + 2\phi_1) \cos(\Psi) - 2\rho_2 \sin(\Psi) \sin(2s + 2\phi_1) \quad (21)$$

It is clearly seen that as soon as $\Psi \neq 0, \pi$ the concentration field loses its axial symmetry (generated by second harmonic), which results into a curved trajectory, as shown below. The existence of a non trivial fixed point for Ψ (Eq. (19c)) requires

$$\beta_2\rho_1^2 - 2\beta_1\rho_2^2 = 0 \quad (22)$$

This means that β_1 and β_2 must have the same sign (as already discussed before). Setting $\dot{\rho}_1 = \dot{\rho}_2 = 0$ in (19a)-(19b) determines ρ_1 and ρ_2 as a function of $\cos(\Psi)$, and using (19c) leads to a closed equation for Ψ . The explicit condition for fixed point of Ψ in Eq.(22), which relates the coefficients $\beta_i, \gamma_i \dots$ entering the model, is given in [31]. A non trivial fixed point of (19c), yields from Eq.(20) $\dot{\phi}_1 = \beta_1\rho_2^0 \sin(\Psi^0)$ ('0' refers to the fixed point solution). This entails that

$$\phi_1 = \beta_1\rho_2^0 \sin(\Psi^0)t \equiv v_d t \quad (23)$$

From Eq. (21) we see that the concentration field drifts in time sideways along the bead surface with velocity v_d . The bead velocity $\mathbf{v}(t)$ is related to $c(s, t)$ and possibly its gradients. For example, for phoretic particles[24] $\mathbf{v}(t) \sim \int_0^{2\pi} \nabla_s c(s, t) ds \sim [-Re(C_1), Im(C_1)]$. This expression holds whenever \mathbf{v} is a linear function of c and its gradients (see another example [3]). The bead Cartesian coordinates are then given by

$$x \sim \frac{\rho_1^0}{v_d} \sin(v_d t), \quad y \sim -\frac{\rho_1^0}{v_d} \cos(v_d t) \quad (24)$$

This is the equation of a circle with radius $R_{circle} \sim \rho_1^0/v_d$.

One can express from Eq. (19a)-(19b) ρ_1^0 and ρ_2^0 as a function of $\cos(\Psi)$, and plugging this into Eq.(19c) we obtain $\dot{\Psi} = G[\cos(\Psi)] \sin(\Psi)$, where the function G is listed in [31]. In the vicinity of the emergence of the circular trajectory G is small, and we obtain to leading order (see [31])

$$\dot{\Psi} = \frac{(\sigma_2 - \sigma_2^c)}{b} \Psi - \xi \Psi^3 \quad (25)$$

with b, ξ positive quantities, functions of the parameters entering (19a)-(19c) (see [31]). Setting, for example, all coefficients to unity, except σ_2 , serving as a single control parameter, we find $\sigma_2^c \simeq -0.09$ (and $b \simeq 0.38, \xi \simeq 7.7$), meaning that at criticality the second harmonic is almost neutral (small growth rate). The bifurcation to circular trajectory is of supercritical nature, and the phase Ψ^0 behaves close to the critical point as $(\sigma_2 - \sigma_2^c)^{1/2}$. According to (23) and (24), the radius of the circle diverges at the critical point of circular trajectory

$$R_{circle} \sim \frac{1}{(\sigma_2 - \sigma_2^c)^{1/2}} \quad (26)$$

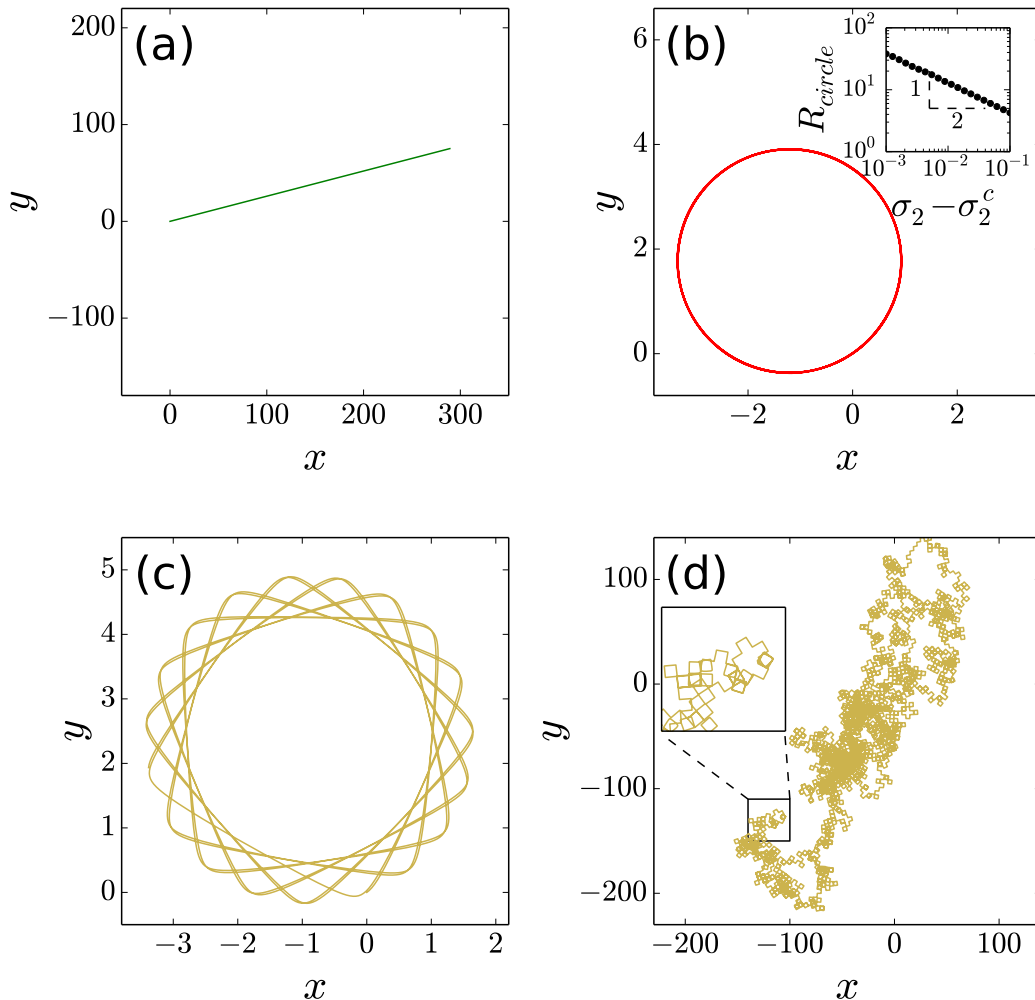


FIG. 1. Swimming patterns as σ_2 increases (growth rate of second harmonic). (a) Straight ($\sigma_2 = -1$), (b) circular ($\sigma_2 = 0.1$; inset shows scaling of circle radius close to criticality confirming prediction (Eq. (26)), (c) precession ($\sigma_2 = 0.4$), and (d) chaotic trajectories ($\sigma_2 = 1.2$).

Numerical solution of (19a)-(19c) confirms this prediction (Fig. 1). This scaling is observed for light-sensitive colloidal swimmers [32], and is expected to be generic. Numerical solution of (19a)-(19c) reveals a complex dynamics ranging from straight trajectories to chaotic ones. To illustrate this, we have set all parameters to unity, and varied σ_2 from negative to positive (by keeping σ_2 small enough for higher order harmonics to play a minor role).

Figure 1 shows a typical swimming pattern, going from straight, circular, precession, to an apparently erratic motion. This last motion (chaos) bears strong resemblance with the run-tumble dynamics, having a persistent random walk feature. We measure the mean square displacement

$$\text{MSD}(\tau) = \langle \Delta x^2(\tau) \rangle = \langle \|\mathbf{x}(t+\tau) - \mathbf{x}(t)\|^2 \rangle,$$

where $\mathbf{x}(t)$ is the location of the particle at time t and $\langle \cdot \rangle$ denotes the average along the entire trajectory. Figure 2 reports the MSD. At short time we have a ballistic motion, whereas for longer times, a de-correlation process due to chaotic turns of velocity direction leads to a MSD proportional to τ^κ , where κ depends on model parameters, yielding both diffusive and sub-diffusive regimes (Fig. 2). Actually, it is not obvious that a chaotic motion is equivalent (at long time) to normal diffusion. There are several chaotic maps yielding anomalous diffusion [33].

Extension to 3D. As in 2D the 3D model relies only on two harmonics of the concentration field, c_i and c_{ij} , where c_i is a 3D vector and c_{ij} is a 3D symmetric traceless tensor. The particle is taken as a unit sphere with a concentration

$$c(\mathbf{r}) = c_i r_i + c_{ij} r_i r_j. \quad (27)$$

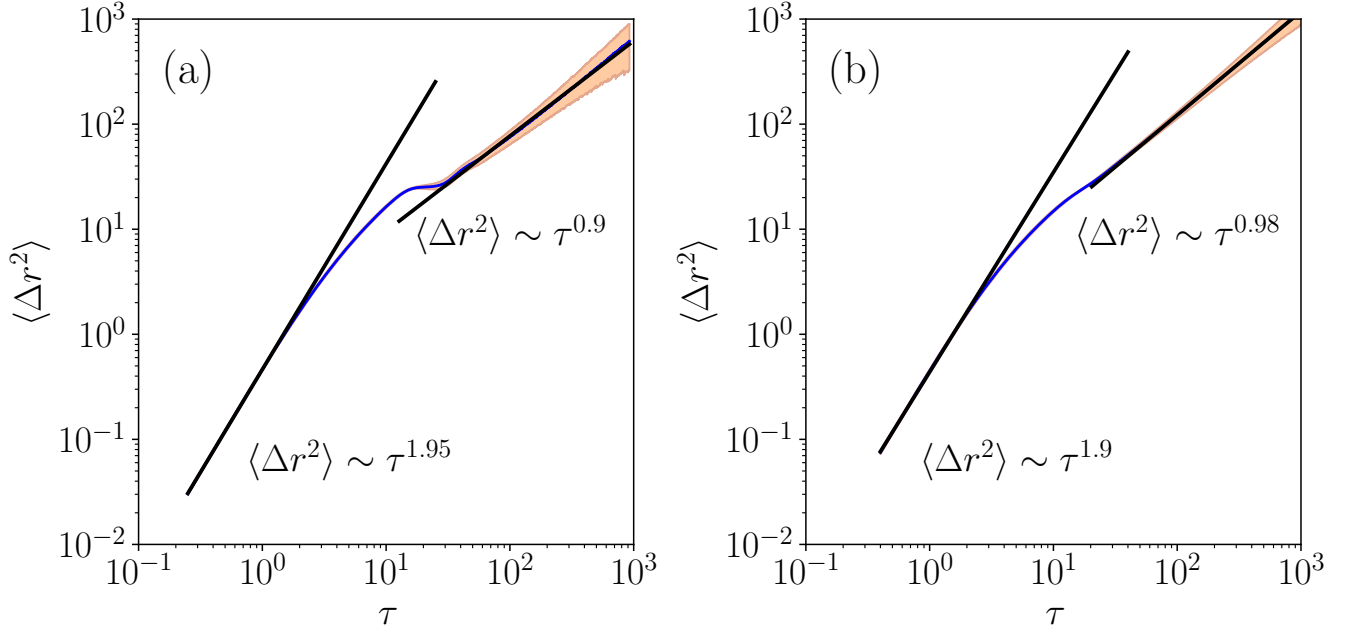


FIG. 2. Mean square displacement for (a) $\sigma_2 = 1.0$ and (b) $\sigma_2 = 1.2$. The shaded region corresponds to the standard deviation in MSD.

where r_i is the i th component of position vector on the particle surface. We propose the following system (see Supplemental Materials):

$$\dot{c}_i = \sigma_1 c_i + \alpha_1 c_j^2 c_i + \beta_1 (c_k^2 c_{ij} c_j - c_j c_k c_{jk} c_i) \quad (28a)$$

$$\dot{c}_{ij} = \sigma_2 c_{ij} + \beta_2 (c_i c_j - \delta_{ij} c_k^2 / 3). \quad (28b)$$

All terms written above are consistent with symmetry (three rotations). System (28a,b) leaves the evolution of the norm of c_i independent of c_{ij}

$$c_i \dot{c}_i = \sigma_1 c_i^2 + \alpha_1 (c_i^2)^2. \quad (29)$$

This choice is not necessary, but allows for a complete analytical handling (results are unaffected by this choice (see below)). This is the classical form of a pitchfork bifurcation. We assume $\alpha_1 < 0$ (supercritical bifurcation). With this choice, we obtain that for $\sigma_1 < 0$ the stable solution is $c_i^2 = 0$, which corresponds to a non-motile case. For $\sigma_1 > 0$, the stable solution is

$$c_i^2 = -\sigma_2 / \alpha_1, \quad (30)$$

which corresponds to a motile solution (recall that the swimming speed v_i is proportional to c_i). Since the norm dynamics of c_i is decoupled, we assume below that the norm of c_i has already reached its stationary value defined by Eq. (30) (in 2D we have actually shown that for circular motion amplitudes ρ_1 and ρ_2 are constants). As we have seen in 2D a circular trajectory leads to a fixed concentration spot moving along the particle periphery. Instead of using the dynamics of phases (ϕ_1 and ϕ_2) as in 2D, we find it more convenient in 3D to follow another approach. The idea is to find if there is a co-rotating frame in which the concentration spot would be steady. Rotation of a spot along the sphere requires some symmetry-breaking. For the straight motion (say along x) the spot possesses axial symmetry around that axis. A first obvious breaking of this symmetry leaves a single mirror of symmetry containing x -axis; we take it to be $x - y$ plane. We will see that the concentration spot will spontaneously move along the equator, and the particle will follow a circular path. The next broken symmetry is the $x - y$ mirror, which will make the spot to move along a closed trajectory, distinct from equator, and the particle follows a helical path. It is convenient to solve our system (28a)-(28b) in the co-moving frame with angular velocity ω (to be determined) of concentration spot. The left hand side of (28a)-(28b) become (see [31]) $\dot{c}_i + \varepsilon_{ijk} \omega_j c_k$ (ε is Levi-Civita symbol) and $\dot{c}_{ij} + \varepsilon_{ikl} \omega_k c_{lj} + \varepsilon_{jkl} \omega_k c_{li}$. Then setting $\omega_i = \beta_1 \varepsilon_{ijk} c_j c_k c_l$ cancels β_1 term in (28a), and we are then left with equation of c_{ij} only.

We first consider the case with $c_{xz} = c_{yz} = 0$ (we assume $x - y$ plane symmetry). The only non-zero ω_i is $\omega_z = \beta_1 c_j^2 c_{xy}$. Analysis of c_{xy} equation shows a stable nontrivial fixed point for $(c_i^2)^2 > \sigma_2^2 / (\beta_1 \beta_2)$. Because only

$\omega_z \neq 0$ the spot rotates along the equator (and so does vector c_i), and the particle follows a circular path. We subsequently analyze linear stability of this solution (see [31]), by allowing modes breaking $x - y$ mirror symmetry (meaning c_{xz} and c_{yz} non zero). A straightforward eigenvalue problem shows that $x - y$ mirror symmetry is lost for $(c_i^2)^2 > 3\sigma_2^2(\beta_1\beta_2)$, and we find (besides ω_z) $\omega_x = \beta_1 c_i^2 c_{yz}$ (an appropriate choice of z -axis allows to set $c_{xz} = 0$), meaning that as soon as $c_{yz} \neq 0$, the spot moves along a circle different from equator and the particle follows a helical path (Fig. 3).

To highlight the genericity of the presented results, we write below the evolution equations for the first and second harmonics based on symmetry only (invariance under 3D rotations), without adopting the special form (28b) expressed by the β_1 term. To the leading order we have

$$\dot{c}_i = \sigma_1 c_i + \alpha_1 c_j^2 c_i + \beta_1 c_{ij} c_j \quad (31a)$$

$$\dot{c}_{ij} = \sigma_2 c_{ij} + \beta_2 (c_i c_j - \delta_{ij} c_k^2 / 3). \quad (31b)$$

Figure 3 shows the full numerical result of this model which captures the analytical results.

Before concluding this section, some remarks are in order. We have written here the two harmonic equations based on symmetries. We have shown how to derive in 2D the two harmonic equations from an explicit phoretic model (more details can be found in [30], exhibiting both qualitative and quantitative agreements with the full model). The same strategy could be adopted in 3D without additional conceptual complications. Our goal was to highlight that two harmonics are sufficient to capture the essential features, and that symmetries can dictate the general form of the equations. The structure of the explicit phoretic model adopted here calls for an important remark, however. For the 3D version of the phoretic model adopted here, it has been shown by Rednikov et al.[34] and by Morozov and Michelin [35] that the swimming speed V_0 does not behave as the square root with distance from threshold (as follows from our study), but has a linear behavior. More precisely, for $Pe < Pe_1$, $V_0 = 0$ and $|V_0| \sim Pe - Pe_1$ for $Pe > Pe_1$. We note in passing that Morozov and Michelin [35] called this bifurcation *transcritical*, but in fact this is still a pitchfork bifurcation, albeit non classical, since the solution $V_0 = 0$ becomes unstable for $Pe > Pe_1$ in favor of two symmetric solutions, $V_0 \sim \pm(Pe - Pe_1)$. We should refer to this bifurcation as a singular pitchfork bifurcation; it is definitely not a transcritical bifurcation [35] which requires that a fixed point branch (here the non motile state) exchanges its stability with the other fixed point branch (motile state) at their crossing junction. We have considered recently a simplified version of the phoretic model and found an exact analytical solution [36] which confirms the singular nature, in that $|V_0| \sim Pe - Pe_1$ for $Pe > Pe_1$. We have shown that this singular behavior occurs only for an infinite system size (be it in 2D or 3D), whereas for a finite size (but arbitrary large) the bifurcation is a classical pitchfork bifurcation, in that $V_0 \sim (Pe - Pe_1)^{1/2}$. This implies that our spirit of regular expansion in power series of harmonic amplitudes (C_1 and C_2) is legitimate for a finite size. In addition, we have shown that the singular behavior for infinite size is only present in the particular phoretic model presented here and considered by Rednikov et al.[34] and Morozov and Michelin [35]. Indeed, if a slightly different version of the model is adopted [36], in which it is supposed that the emitted solute is, besides advection and diffusion, consumed at a certain frequency (giving rise, for example, to some product, not necessarily for interest), then the singular nature of the bifurcation for infinite systems is suppressed (even for an infinitesimal consumption rate); the bifurcation becomes of classical pitchfork bifurcation. Nevertheless, the works of Rednikov et al.[34] and Morozov and Michelin [35] have a merit of pointing out a non trivial singular nature of bifurcation, rarely encountered in classical nonequilibrium systems undergoing bifurcations (such as Bénard and Marangoni convection, Turing systems, crystal growth... which have been a focus of nonlinear community for decades). The singular nature of the bifurcation means that the radius of convergence of expansions in powers of amplitudes of harmonics goes to zero at the bifurcation point. This raises an important question of how to properly cope a priori, for a given nonlinear model, with the existence of singular bifurcations in a proper manner. We have provided very recently a framework along this line [36].

Conclusion. The model has identified the fact that locomotory complexity leading to diverse trajectories can be captured on the basis of symmetries and nonlinear interactions, lending evidence to its universality. The model can be adopted for any motion fueled by a chemical field, a prominent and vast field of research is mammalian cell motility, which is known to be dictated by myosin and actin kinetics. The model can be effective not only for spherically shaped motile entities, but also for any shape as long as the shape of the cell can be reconstructed from the chemical field. The model can also find application in embryonic development. Underlying the multicellular choreography is the actomyosin cytoskeleton dynamics, leading to the propagation of localized concentration pulses[37, 38] affecting cell rearrangement. This study also opens up new perspectives to tackle motility from a novel angle. Indeed, it should incite analytical derivation of simple nonlinear equations (as studied here) from different explicit examples of motility. This will allow linking the phenomenological coefficients used here to biophysical and chemical parameters of a motile system, in order to determine the conditions of manifestation, or the lack thereof, of complex motions in parameter space, without resorting to the computationally expensive solution of the full basic model, which involves reaction-diffusion-advection with long range hydrodynamics.

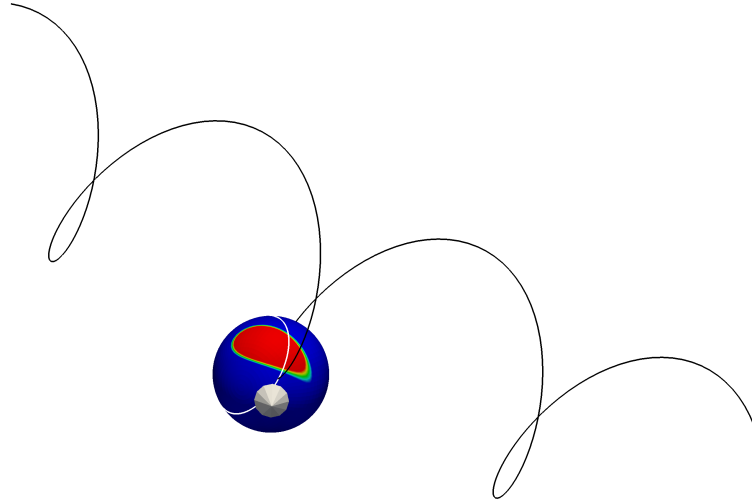
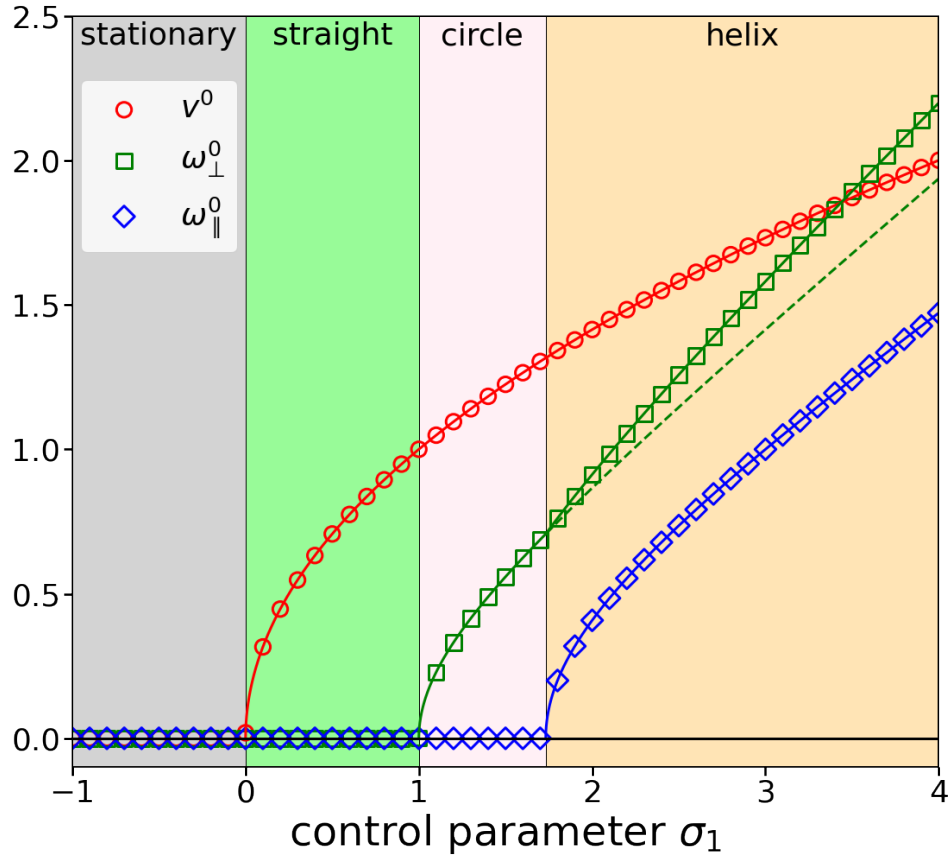


FIG. 3. Top: Bead velocity showing series of bifurcations from straight, circular to helical motion. The components of angular velocity along the velocity and orthogonal to it are shown as ω_{\parallel}^0 and ω_{\perp}^0 , respectively. Solid lines refer to analytical solution and symbols to numerical ones. Bottom: Bead trajectory showing helical path and a concentration spot following a circle (white) outside the equator.

We thank CNES (Centre National d'Etudes Spatiales) (C.M. S. M. R. and A.F.) for a financial support and for having access to experimental data, and the French-German university program "Living Fluids" (grant CFDA-Q1-14)

(C.M., A.F. and S. R.) for a financial support

- [1] Nicholas P Barry and Mark S Bretscher, “Dictyostelium amoebae and neutrophils can swim,” *Proceedings of the National Academy of Sciences* **107**, 11376–11380 (2010).
- [2] Patrick R. O’Neill, Jean A. Castillo-Badillo, Xenia Meshik, Vani Kalyanaraman, Krystal Melgarejo, and N. Gautam, “Membrane flow drives an adhesion-independent amoeboid cell migration mode,” *Developmental Cell* **46**, 9 – 22.e4 (2018).
- [3] A. Farutin, J. Etienne, C. Misbah, and P. Récho, “Crawling in a fluid,” *Phys. Rev. Lett.* **123**, 118101 (2019).
- [4] Laurene Aoun, Paulin Negre, Alexander Farutin, Nicolas Garcia-Seyda, Mohd Suhail Rivzi, Remi Galland, Alpee Michelot, Xuan Luo, Martine Biarnes-Pelicot, Claire Hivroz, Salima Rafai, Jean-Baptiste Sibaret, Marie-Pierre Valignat, Chaouqi Misbah, and Olivier Theodoly, “Mammalian amoeboid swimming is propelled by molecular and not protrusion-based paddling in lymphocytes,” *Biophys. J.* **119**, 1157–1177 (2020).
- [5] Francesco Mori, Pierre Le Doussal, Satya N. Majumdar, and Grégory Schehr, “Universal survival probability for a d -dimensional run-and-tumble particle,” *Phys. Rev. Lett.* **124**, 090603 (2020).
- [6] L Angelani, R Di Leonardo, and M Paoluzzi, “First-passage time of run-and-tumble particles,” *The European Physical Journal E* **37**, 59 (2014).
- [7] Jean-Fran çois Rupprecht, Olivier Bénichou, and Raphael Voituriez, “Optimal search strategies of run-and-tumble walks,” *Phys. Rev. E* **94**, 012117 (2016).
- [8] O. Bénichou, C. Loverdo, M. Moreau, and R. Voituriez, “Intermittent search strategies,” *Rev. Mod. Phys.* **83**, 81–129 (2011).
- [9] Marco Polin, Idan Tuval, Knut Drescher, J. P. Gollub, and Raymond E. Goldstein, “Chlamydomonas swims with two “gears” in a eukaryotic version of run-and-tumble locomotion,” *Science* **325**, 487–490 (2009), <https://science.sciencemag.org/content/325/5939/487.full.pdf>.
- [10] H. S. Jennings, “On the significance of spiral swimming of organisms,” *Am. Soc. Natural.* **35**, 369 (1901).
- [11] Ingmar H. Riedel, Karsten Kruse, and Jonathon Howard, “A self-organized vortex array of hydrodynamically entrained sperm cells,” *Science* **309**, 300–303 (2005), <https://science.sciencemag.org/content/309/5732/300.full.pdf>.
- [12] Saikat Jana, Soong Ho Um, and Sunghwan Jung, “Paramecium swimming in capillary tube,” *Physics of fluids* **24**, 041901 (2012).
- [13] Howard C Berg, *Random walks in biology* (Princeton University Press, 1993).
- [14] Michael E Cates and Julien Tailleur, “When are active brownian particles and run-and-tumble particles equivalent? consequences for motility-induced phase separation,” *EPL (Europhysics Letters)* **101**, 20010 (2013).
- [15] V. B. Shenoy, D. T. Tambe, A. Prasad, and J. A. Theriot, “A kinematic description of the trajectories of listeria monocytogenes propelled by actin comet tails,” *Proceedings of the National Academy of Sciences* **104**, 8229–8234 (2007).
- [16] Carsten Krüger, Gunnar Klös, Christian Bahr, and Corinna C Maass, “Curling liquid crystal microswimmers: A cascade of spontaneous symmetry breaking,” *Phys. Rev. Lett.* **117**, 048003 (2016).
- [17] Hartmut Löwen, “Chirality in microswimmer motion: From circle swimmers to active turbulence,” *The European Physical Journal Special Topics* **225**, 2319–2331 (2016).
- [18] Mariko Suga, Saori Suda, Masatoshi Ichikawa, and Yasuyuki Kimura, “Self-propelled motion switching in nematic liquid crystal droplets in aqueous surfactant solutions,” *Phys. Rev. E* **97**, 062703 (2018).
- [19] Narinder Narinder, Clemens Bechinger, and Juan Ruben Gomez-Solano, “Memory-induced transition from a persistent random walk to circular motion for achiral microswimmers,” *Phys. Rev. Lett.* **121**, 078003 (2018).
- [20] Ziane Izri, Marjolein N Van Der Linden, Sébastien Michelin, and Olivier Dauchot, “Self-propulsion of pure water droplets by spontaneous marangoni-stress-driven motion,” *Phys. Rev. Lett.* **113**, 248302 (2014).
- [21] W. F. Hu, T. S. Lin, S. Rafai, and C. Misbah, “Chaotic swimming of phoretic particles,” *Phys. Rev. Lett.* **123**, 238004 (2019).
- [22] E. Lauga, W. R. DiLuzio, G. M. Whitesides, and H. A. Stone, “Swimming in circles: Motion of bacteria near solid boundaries,” *Biophys. J.* **105**, 069401 (2006).
- [23] S. Michelin, E. Lauga, and D. Bartolo, “Spontaneous autophoretic motion of isotropic particles,” *Phys. Fluids* **25**, 061701 (2013).
- [24] Matvey Morozov and Sébastien Michelin, “Nonlinear dynamics of a chemically-active drop: From steady to chaotic self-propulsion,” *The Journal of chemical physics* **150**, 044110 (2019).
- [25] Maximilian Schmitt and Holger Stark, “Swimming active droplet: A theoretical analysis,” *EPL (Europhysics Letters)* **101**, 44008 (2013).
- [26] Rhoda J Hawkins, Renaud Poincloux, Olivier Bénichou, Matthieu Piel, Philippe Chavier, and Raphaël Voituriez, “Spontaneous contractility-mediated cortical flow generates cell migration in three-dimensional environments,” *Biophysical journal* **101**, 1041–1045 (2011).
- [27] A. C. Callan-Jones, V. Ruprecht, S. Wieser, C. P. Heisenberg, and R. Voituriez, “Cortical flow-driven shapes of nonadherent cells,” *Phys. Rev. Lett.* **116**, 028102 (2016).
- [28] D. Sondak, C. Hawley, S. Heng, R. Vinsonhaler, E. Lauga, and J.-L. Thiffeault, “Can phoretic particles swim in two dimensions?” *Phys. Rev. E* **94**, 062606 (2016).
- [29] J.R. Blake, “Self propulsion due to oscillations on the surface of a cylinder at low reynolds number,” *Bulletin of the*

- Australian Mathematical Society **5**, 255–264 (1971).
- [30] Alexander Farutin, Mohd Suhail Rizvi, Wei Fan Hu, Te Sheng Lin, Salima Rafai, and Chaouqi Misbah, “A reduced model for a phoretic swimmer,” arXiv:2112.12023 (2021).
 - [31] See supplemental material at [URL will be inserted by publisher].
 - [32] N Narinder, Clemens Bechinger, and Juan Ruben Gomez-Solano, “Memory-induced transition from a persistent random walk to circular motion for achiral microswimmers,” *Phys. Rev. Lett.* **121**, 078003 (2018).
 - [33] T. Geisel and J. Nierwetberg, “Onset of diffusion and universal scaling in chaotic systems,” *Phys. Rev. Lett.* **48**, 7–10 (1982).
 - [34] Alexei Ye Rednikov, Yuri S Ryazantsev, and Manuel G Velarde, “Drop motion with surfactant transfer in a homogeneous surrounding,” *Physics of Fluids* **6**, 451–468 (1994).
 - [35] Matvey Morozov and Sébastien Michelin, “Self-propulsion near the onset of marangoni instability of deformable active droplets,” *Journal of Fluid Mechanics* **860**, 711–738 (2019).
 - [36] Alexandr Farutin and Chaouqi Misbah, “Singular bifurcations: a regularization theory,” arXiv:2112.12094 (2021).
 - [37] Negro, G., Lamura, A., Gonnella, G., and Marenduzzo, D., “Hydrodynamics of contraction-based motility in a compressible active fluid,” *EPL* **127**, 58001 (2019).
 - [38] Guy B Blanchard, Jocelyn Étienne, and Nicole Gorfinkiel, “From pulsatile apicomedial contractility to effective epithelial mechanics,” *Current Opinion in Genetics & Development* **51**, 78 – 87 (2018), developmental mechanisms, patterning and evolution.